Appendix

Serine and one-carbon metabolism is required for HIF mediated protection against retinopathy of prematurity

Charandeep Singh[1], George Hoppe[1], Vincent Tran[1], Leah McCollum[1], Youstina Bolok[1], Weilin Song[1], Amit Sharma[1], Henri Brunengraber[2], and Jonathan E Sears[1,3,*]

[1]Cole Eye Institute, Cleveland Clinic, 9500 Euclid Avenue, Cleveland Ohio 44195

[2]Department of Nutrition, Case Western Reserve University, Cleveland, OH 44109

[3]Cellular and Molecular Medicine, 9500 Euclid Avenue, Cleveland Ohio 44195

*Corresponding Author: Sears JE, Cole Eye institute, Cleveland Clinic, 9500 Euclid Avenue, Cleveland Ohio 44195 Email: searsj@ccf.org

Supplementary tables -4

Supplementary figures-6

Appendix Table S1 Systems levels analysis of pathways affected by Hyperoxia vs Hyperoxia+Roxadustat of plasma metabolome in positive ionization mode of LC-MS/MS data.

Pathway	Overlapping putative metabolites	p-values
1,25-dihydroxyvitamin D3 biosynthesis/ Calcitriol	100.00%	1.80E-03
folate polyglutamylation	100.00%	4.70E-03
glycine biosynthesis III	100.00%	4.70E-03
citrulline degradation	100.00%	3.30E-02
asparagine degradation I	100.00%	3.30E-02
Serine degradation II	100.00%	3.30E-02
L-serine degradation	100.00%	3.30E-02
N-acetylneuraminate and N-acetylmannosamine degradation	100.00%	3.30E-02
putrescine biosynthesis III	100.00%	3.30E-02
histamine biosynthesis	100.00%	3.30E-02
pyrimidine ribonucleotides interconversion	100.00%	3.30E-02
glycine biosynthesis I	100.00%	3.30E-02
urea cycle	85.70%	1.20E-03
glycine betaine degradation	85.70%	1.20E-03
4-hydroxyproline degradation I	83.30%	1.70E-03
citrulline-nitric oxide cycle	83.30%	1.70E-03
arginine biosynthesis IV	80.00%	1.10E-03
asparagine biosynthesis I	80.00%	3.40E-03
citrulline biosynthesis	77.80%	1.20E-03
proline biosynthesis II (from arginine)	75.00%	1.60E-03
alanine degradation III	75.00%	1.20E-02
glutamine degradation II	75.00%	1.20E-02
aspartate degradation II	75.00%	1.20E-02
glutathione biosynthesis	75.00%	1.20E-02
uridine-5-phosphate biosynthesis	75.00%	1.20E-02
alanine biosynthesis II	75.00%	1.20E-02
aspartate biosynthesis	75.00%	1.20E-02
arginine degradation VI (arginase 2 pathway)	71.40%	2.60E-03
tRNA charging pathway	70.00%	9.70E-04
histidine degradation III	66.70%	6.70E-03
putrescine degradation III	66.70%	6.70E-03
arginine degradation I (arginase pathway)	66.70%	6.70E-03
phenylalanine degradation III	62.50%	4.40E-03

β-alanine degradation I	60.00%	2.80E-02
4-aminobutyrate degradation IV	60.00%	2.80E-02
glutathione-mediated detoxification	60.00%	2.80E-02
glycine degradation (creatine biosynthesis)	60.00%	2.80E-02
folate transformations I	60.00%	2.80E-02
folate transformations II (plants)	60.00%	2.80E-02
salvage pathways of pyrimidine deoxyribonucleotides	60.00%	2.80E-02
proline biosynthesis II	60.00%	2.80E-02
creatine biosynthesis	57.10%	1.30E-02
glutamate degradation IV	50.00%	2.60E-02
lysine degradation II	44.40%	4.80E-02
purine and pyrimidine metabolism	41.70%	4.20E-02

Appendix Table S2 Systems levels analysis of pathways affected by Hyperoxia vs Hyperoxia+Roxadustat of plasma metabolome in negative ionization mode of LC-MS/MS data.

Pathway	Overlapping putative metabolites	p-values
histidine degradation III	100.00%	3.50E-03
histamine degradation	100.00%	3.50E-03
cysteine biosynthesis II	100.00%	4.10E-03
cysteine biosynthesis/homocysteine degradation	100.00%	4.10E-03
ketone oxidation	100.00%	1.20E-02
L-arabinose degradation II	100.00%	1.20E-02
ketolysis	100.00%	1.20E-02
citrulline degradation	100.00%	4.80E-02
asparagine degradation I	100.00%	4.80E-02
ketogenesis	100.00%	4.80E-02
aerobic respiration -- electron donor II	100.00%	4.80E-02
histamine biosynthesis	100.00%	4.80E-02
ketogenesis	100.00%	4.80E-02
coenzyme A biosynthesis	100.00%	4.80E-02
molybdenum cofactor (sulfide) biosynthesis	100.00%	4.80E-02
urea cycle	85.70%	4.20E-03
citrulline-nitric oxide cycle	83.30%	5.70E-03
arginine biosynthesis IV	80.00%	3.60E-03
asparagine biosynthesis I	80.00%	1.00E-02

citrulline biosynthesis	77.80%	4.20E-03
proline biosynthesis II (from arginine)	75.00%	5.50E-03
methylglyoxal degradation VI	75.00%	2.60E-02
NAD biosynthesis from 2-amino-3-carboxymuconate semialdehyde	75.00%	2.60E-02
adenosine nucleotides de novo biosynthesis	75.00%	2.60E-02
uracil degradation II (reductive)	75.00%	2.60E-02
arginine degradation VI (arginase 2 pathway)	71.40%	8.70E-03
aerobic respiration -- electron donors reaction list	71.40%	3.10E-02
inosine-5-phosphate biosynthesis II	71.40%	3.10E-02
arginine degradation I (arginase pathway)	66.70%	1.80E-02
glutamate degradation VII	66.70%	2.20E-02
glutamate degradation IV	62.50%	1.40E-02
glutamine degradation II	60.00%	5.00E-02
glutamate degradation III (via 4-aminobutyrate)	60.00%	5.00E-02
L-cysteine degradation III	60.00%	5.00E-02
aspartate degradation II	60.00%	5.00E-02
4-aminobutyrate degradation I	60.00%	5.00E-02
4-aminobutyrate degradation IV	60.00%	5.00E-02
serine biosynthesis	60.00%	5.00E-02
proline biosynthesis II	60.00%	5.00E-02
5-aminoimidazole ribonucleotide biosynthesis I	57.10%	3.10E-02
uridine-5-phosphate biosynthesis	57.10%	3.10E-02
tRNA charging pathway	52.40%	7.90E-03

Appendix Table S3 Systems levels analysis of pathways affected by Hyperoxia vs Hyperoxia+Roxadustat of retina metabolome in positive ionization mode of LC-MS/MS data.

Pathway	Overlapping putative metabolites	p-values
proline degradation II	100.00%	2.10E-03
methylglyoxal degradation II	100.00%	9.30E-03
5-aminoimidazole ribonucleotide biosynthesis II	80.00%	1.60E-03
proline biosynthesis II	80.00%	1.60E-03
arginine degradation VI (arginase 2 pathway)	75.00%	1.10E-03
proline biosynthesis II (from arginine)	75.00%	1.10E-03
alanine degradation III	75.00%	3.80E-03

proline degradation III	75.00%	3.80E-03
alanine biosynthesis II	75.00%	3.80E-03
uracil degradation II (reductive)	75.00%	3.80E-03
citrulline biosynthesis	70.00%	1.00E-03
glutamate degradation IV	66.70%	1.20E-03
tyrosine degradation I	66.70%	2.30E-03
4-hydroxyproline degradation I	66.70%	2.30E-03
4-aminobutyrate degradation IV	66.70%	2.30E-03
glycine degradation (creatine biosynthesis)	66.70%	2.30E-03
5-aminoimidazole ribonucleotide biosynthesis I	66.70%	2.30E-03
glutamine degradation I	66.70%	2.00E-02
methylglyoxal degradation I	66.70%	2.00E-02
glycine biosynthesis III	66.70%	2.00E-02
glutamine biosynthesis II	66.70%	2.00E-02
L-glutamine biosynthesis II (tRNA-dependent)	66.70%	2.00E-02
arginine degradation I (arginase pathway)	62.50%	1.70E-03
tryptophan degradation I (via anthranilate)	60.00%	6.70E-03
UDP-N-acetyl-D-glucosamine biosynthesis II	60.00%	6.70E-03
asparagine biosynthesis I	60.00%	6.70E-03
cysteine biosynthesis II	60.00%	6.70E-03
cysteine biosynthesis/homocysteine degradation	60.00%	6.70E-03
glycine betaine degradation	57.10%	3.50E-03
catecholamine biosynthesis	57.10%	3.50E-03
tRNA charging pathway	52.40%	1.00E-03
lysine degradation II	50.00%	3.20E-03
arginine biosynthesis IV	50.00%	3.20E-03
creatine biosynthesis	50.00%	5.40E-03
β-alanine degradation I	50.00%	1.20E-02
glutamate degradation III (via 4-aminobutyrate)	50.00%	1.20E-02
tryptophan degradation to 2-amino-3-carboxymuconate semialdehyde	50.00%	1.20E-02
4-aminobutyrate degradation I	50.00%	1.20E-02
NAD biosynthesis from 2-amino-3-carboxymuconate semialdehyde	50.00%	1.20E-02
Uridine-5'-phosphate biosynthesis	50.00%	1.20E-02
L-cysteine degradation III	50.00%	3.80E-02
methylglyoxal degradation VI	50.00%	3.80E-02
ketogenesis	50.00%	3.80E-02
ketogenesis	50.00%	3.80E-02
tetrapyrrole biosynthesis II	50.00%	3.80E-02

folate polyglutamylation	50.00%	3.80E-02
pyrimidine ribonucleotides interconversion	50.00%	3.80E-02
histidine degradation III	42.90%	1.90E-02
putrescine degradation III	42.90%	1.90E-02
urea cycle	37.50%	3.00E-02
dopamine degradation	37.50%	3.00E-02
pyridine nucleotide cycling	37.50%	3.00E-02
valine degradation I	36.40%	1.90E-02
phenylalanine degradation III	33.30%	4.50E-02

Appendix Table S4 Systems levels analysis of pathways affected by Hyperoxia vs Hyperoxia+Roxadustat of retina metabolome in negative ionization mode of LC-MS/MS data.

Pathway	Overlapping putative metabolites	p-values
thymine degradation	100.00%	5.50E-03
mevalonate pathway	100.00%	5.50E-03
methionine salvage	100.00%	4.00E-02
lactose degradation III	100.00%	4.00E-02
sucrose degradation	87.50%	1.20E-03
pyrimidine deoxyribonucleosides degradation	83.30%	2.00E-03
guanine and guanosine salvage	75.00%	1.40E-02
trehalose degradation	75.00%	1.40E-02
purine ribonucleosides degradation to ribose-1-phosphate	66.70%	2.50E-03
adenine and adenosine salvage III	66.70%	7.90E-03
purine deoxyribonucleosides degradation	66.70%	7.90E-03

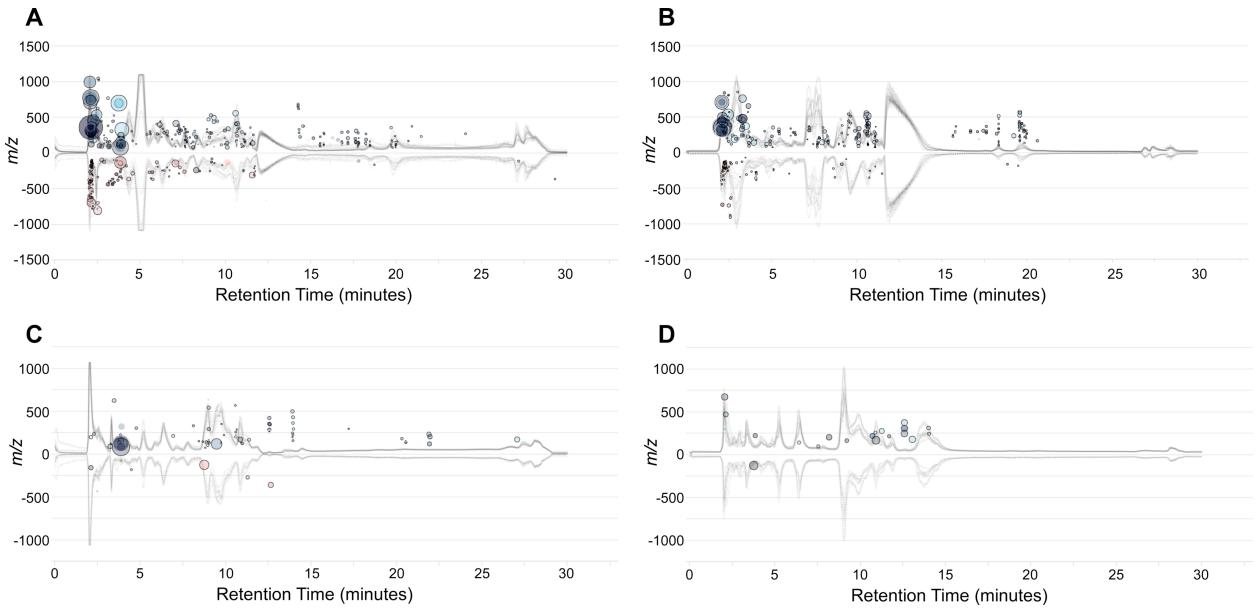

Appendix Figure S1 Metabolite cloud plots depicting metabolite features up and down regulated by the HIF PHi Roxadustat (A-D). Untargeted dd-MS2 data were analyzed using XCMS Online tool and the cloud plots of differentially up or down regulated metabolites were generated. In the cloud plots, different shades of blue represent up-regulated metabolites and different shades of red are the down-regulated metabolites, control hyperoxic (n=6, each group) vs. Roxadustat treated hyperoxic (n=6, each group) C57BL/6 mice samples. Each bubble represent a metabolite feature, where bigger size of the bubble represents higher fold-change and darker color represent lower p-value. Gray-scaled plot in the background represent total-ion chromatograms for each sample. Only metabolite features with p-value ≤ 0.01 and fold change ≥ 1.5 are represented in all four cloud plots. (A) Positive mode plasma samples contained 613 metabolite features. (B) Negative mode plasma samples contained 398 metabolite features. (C) Positive mode plasma samples contained 82 metabolite features. (D) Negative mode retina samples contained 23 metabolite features different between treatment and control groups.

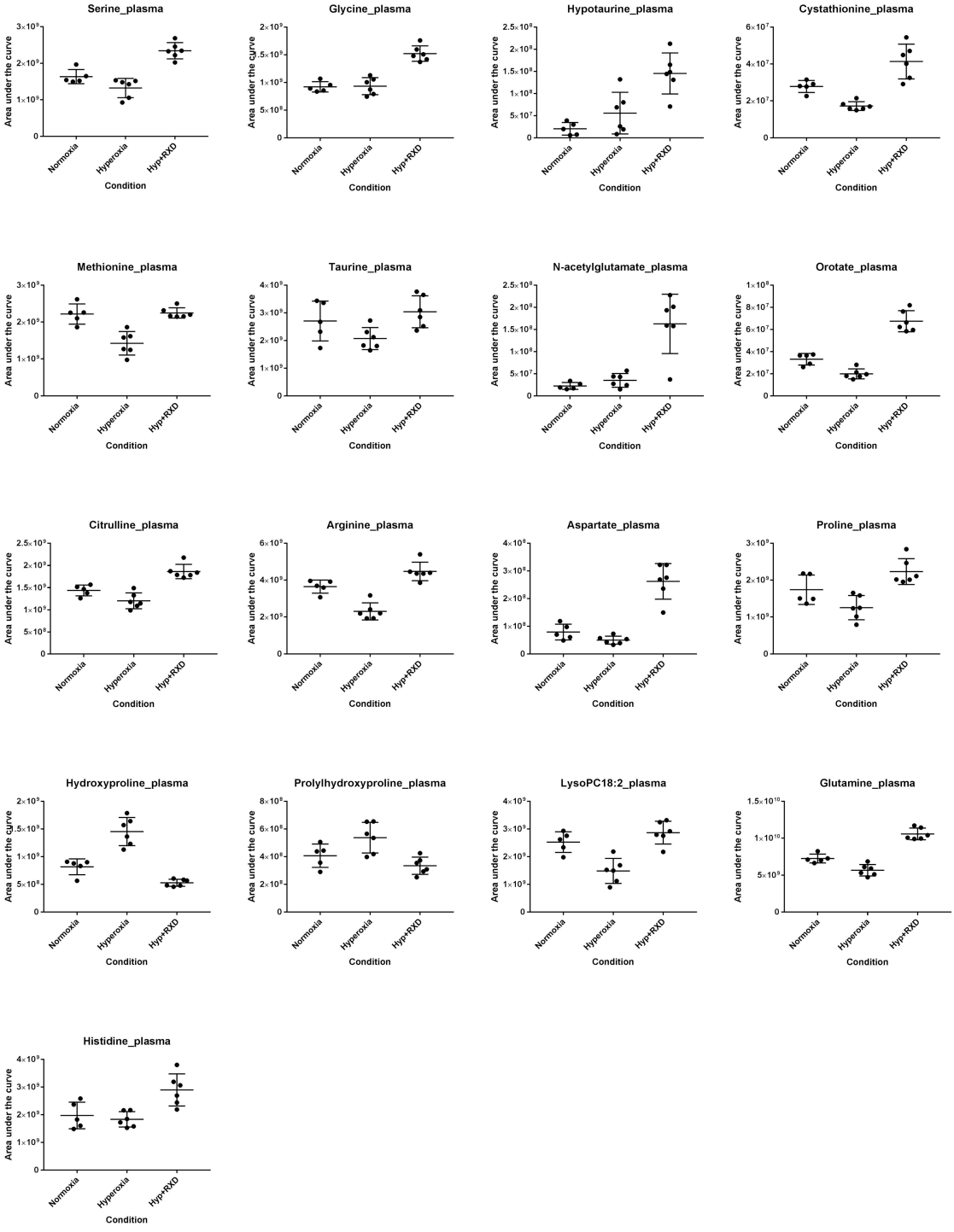

Appendix Figure S2 Box-plots of annotated metabolites from plasma samples demonstrates upregulation of serine 1C and urea pathways.

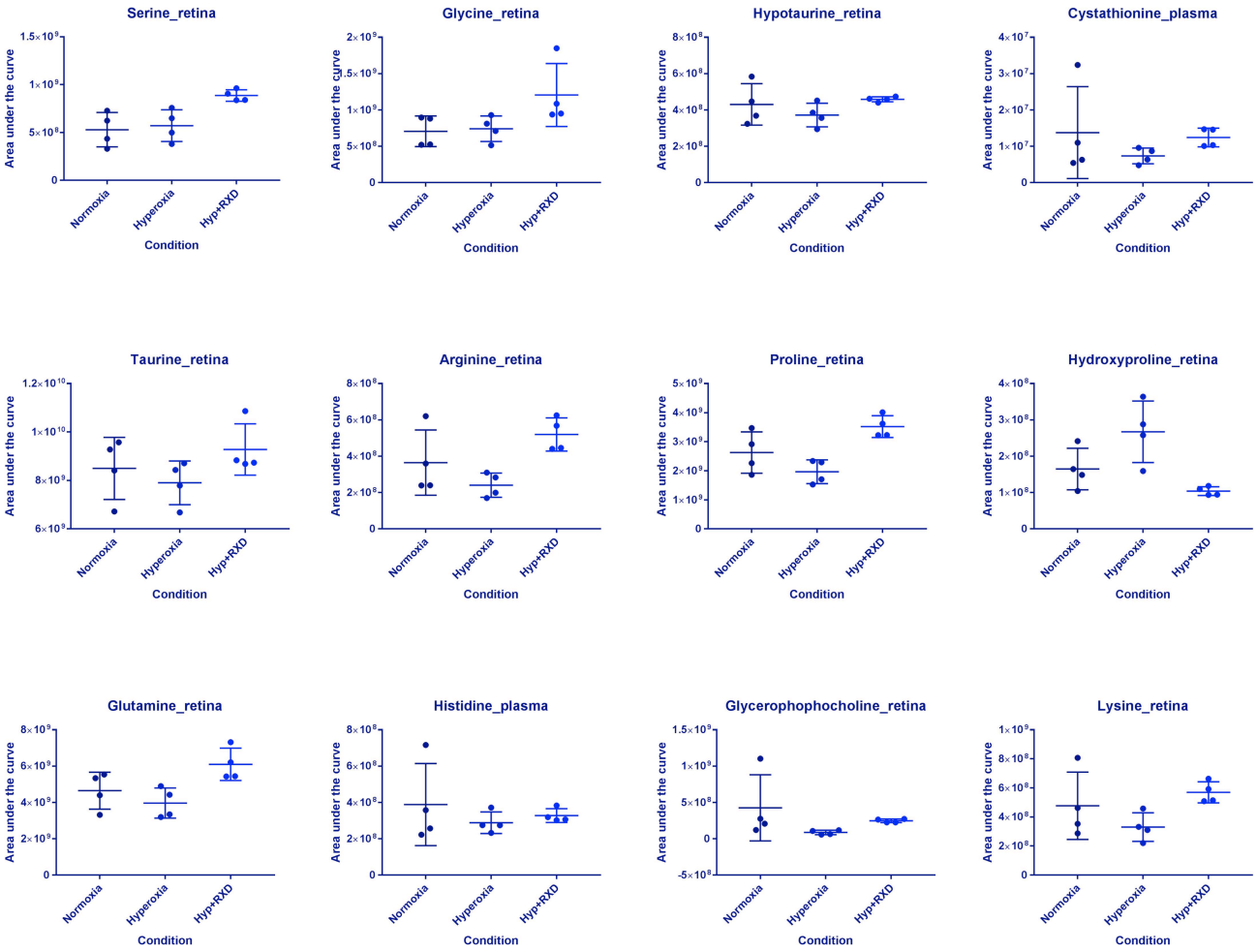

Appendix Figure S3 Box-plots of annotated metabolites from retina samples demonstrates upregulation of serine 1C and urea pathways.

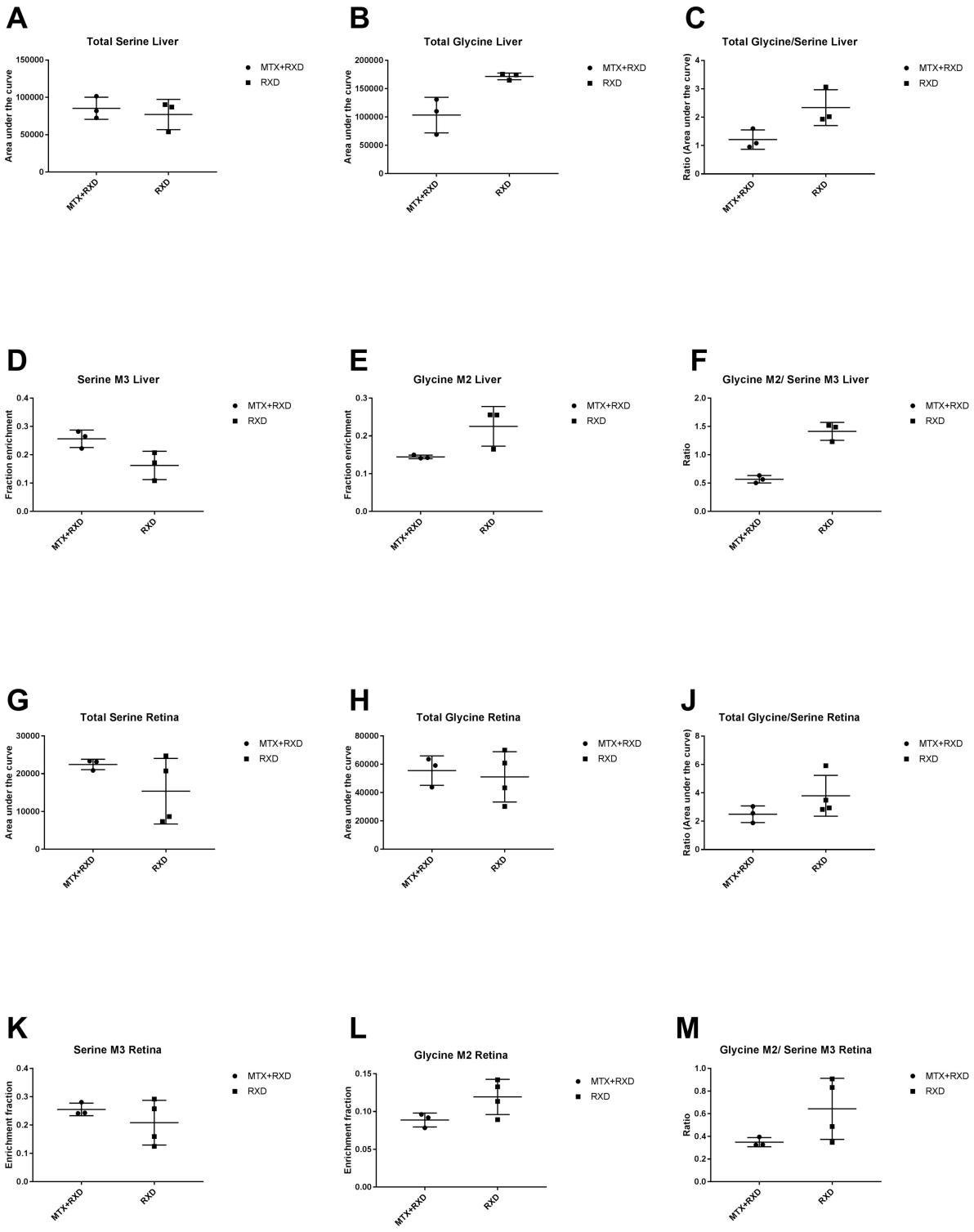
A
Total Serine Liver
Area under the curve
150000
100000
50000
0
MTX+RXD
RXD
MTX+RXD
RXD
B
Total Glycine Liver
Area under the curve
200000
150000
100000
50000
0
MTX+RXD
RXD
MTX+RXD
RXD
C
Total Glycine/Serine Liver
Ratio (Area under the curve)
4
3
2
1
0
MTX+RXD
RXD
MTX+RXD
RXD
D
Serine M3 Liver
Fraction enrichment
0.4
0.3
0.2
0.1
0.0
MTX+RXD
RXD
MTX+RXD
RXD
E
Glycine M2 Liver
Fraction enrichment
0.3
0.2
0.1
0.0
MTX+RXD
RXD
MTX+RXD
RXD
F
Glycine M2/ Serine M3 Liver
Ratio
2.0
1.5
1.0
0.5
0.0
MTX+RXD
RXD
MTX+RXD
RXD
G
Total Serine Retina
Area under the curve
30000
20000
10000
0
MTX+RXD
RXD
MTX+RXD
RXD
H
Total Glycine Retina
Area under the curve
80000
60000
40000
20000
0
MTX+RXD
RXD
MTX+RXD
RXD
J
Total Glycine/Serine Retina
Ratio (Area under the curve)
8
6
4
2
0
MTX+RXD
RXD
MTX+RXD
RXD
K
Serine M3 Retina
Enrichment fraction
0.4
0.3
0.2
0.1
0.0
MTX+RXD
RXD
MTX+RXD
RXD
L
Glycine M2 Retina
Enrichment fraction
0.15
0.10
0.05
0.00
MTX+RXD
RXD
MTX+RXD
RXD
M
Glycine M2/ Serine M3 Retina
Ratio
1.0
0.8
0.6
0.4
0.2
0.0
MTX+RXD
RXD
MTX+RXD
RXD

Appendix Figure S4

Serine to Glycine conversion was decreased in the MTX injected mice. (A) total serine (B) total glycine and (C) total glycine/serine content in mice livers injected with MTX+RXD vs. RXD. Fraction enrichment of (D) M3 serine, (E) M2 glycine and (F) glycine M2/ serine M3 in the mice livers, injected with MTX+RXD vs. RXD. (G) total serine (H) total glycine and (I) total glycine/serine content in mice retina, injected with MTX+RXD vs. RXD. Fraction enrichment of (J) M3 serine, (K) M2 glycine and (L) glycine M2/ serine M3 in the mice livers injected with MTX+RXD vs. RXD MTX, Methotrexate; RXD, Roxadustat.

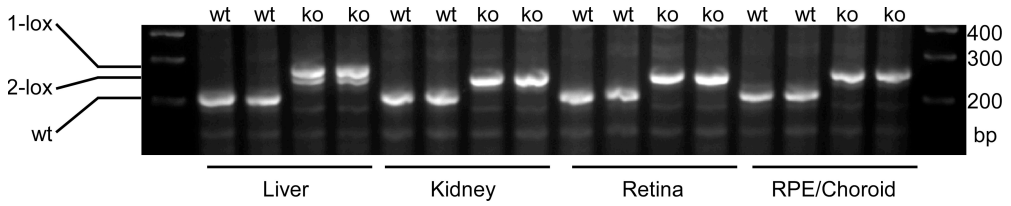

Appendix Figure S5. Liver-specific Cre-induced recombination of HIF1A gene in LHKO mouse strain. Efficient and tissue-specific recombination was confirmed by PCR analysis of genomic DNA extracted from liver, kidney, retina and RPE/choroid of the wt and LHKO mouse. Primers (two forward and one reverse) were designed to amplify the conditional allele (2-lox), recombined allele (1-lox), and WT allele as previously described [Rankin et al, JCI 2007, PMID 17404621]. 1-lox and 2-lox designate the recombined (270-bp) and non-recombined (260-bp) alleles, respectively, and WT allele (240-bp). Following PCR procedure and agarose gel separation of amplicons as described elsewhere [Hoppe et al, AJP 2014, PMID 24731446], only the LHKO liver samples demonstrated the presence of recombined allele (1-lox).

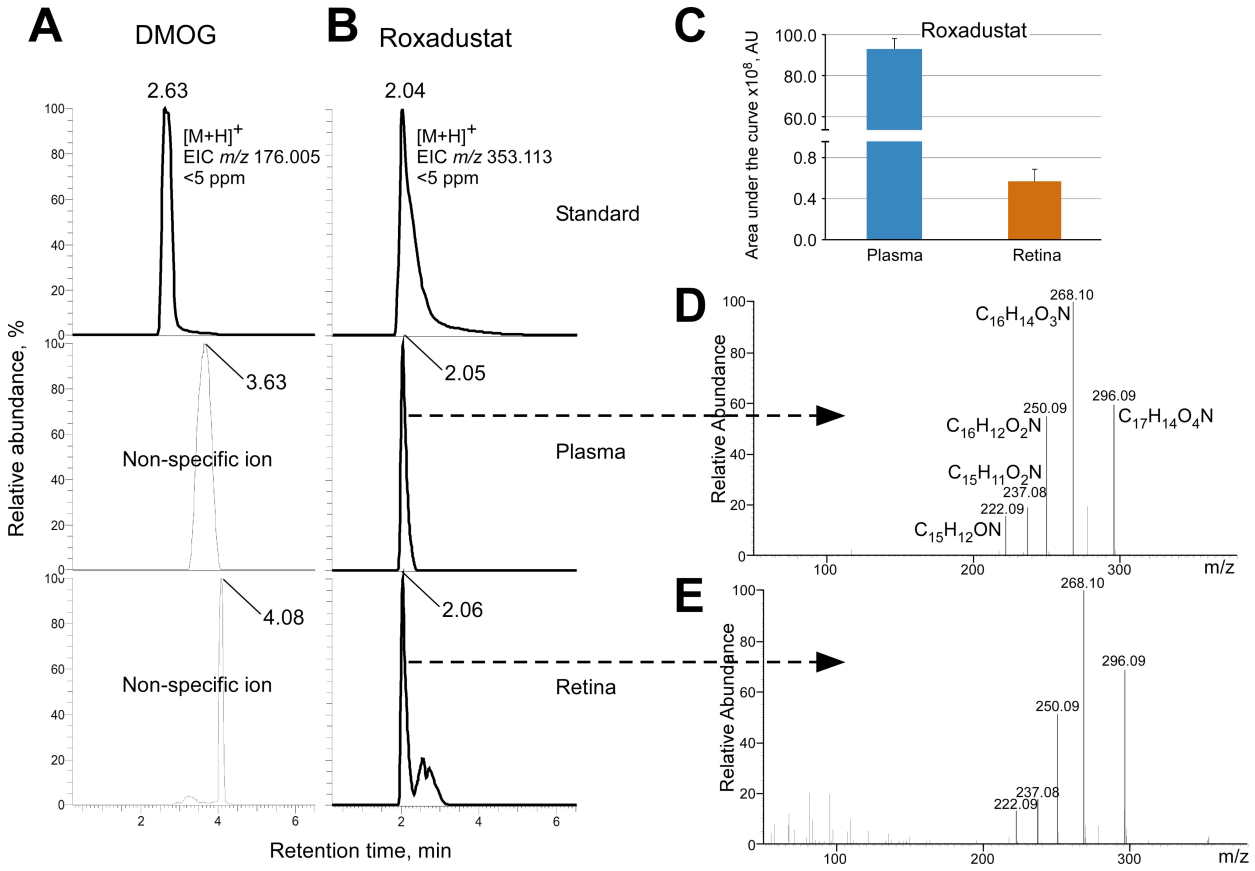

Appendix Figure S6 LCMS1/MS2 of dimethyloxalylglycine (DMOG) versus roxadustat (RXD) demonstrates that DMOG does not enter plasma but RXD does. This provides liver specific action to DMOG when injected intraperitoneally.